

Jean C. Augustinack · Anja Schneider
Eva-Maria Mandelkow · Bradley T. Hyman

Specific tau phosphorylation sites correlate with severity of neuronal cytopathology in Alzheimer's disease

Received: 22 January 2001 / Revised, accepted: 22 May 2001 / Published online: 26 October 2001

© Springer-Verlag 2001

Abstract Microtubule associated protein tau is abnormally phosphorylated in Alzheimer's disease (AD) and aggregates as paired helical filaments (PHFs) in neurofibrillary tangles (NFTs). We show here that the pattern of tau phosphorylation correlates with the loss of neuronal integrity. Studies using 11 phosphorylation dependent tau antibodies and a panel of AD cases of varying severity were evaluated in terms of three stages of neurofibrillary tangle development: (1) pre-neurofibrillary tangle, (2) intra-, and (3) extra-neuronal neurofibrillary tangles. The pretangle state, in which neurons display nonfibrillar, punctate regions in the cytoplasm, somas, dendrites, and nuclei, was observed especially with phospho-tau antibodies TG3 (pT231), pS262, and pT153. Intraneuronal neurofibrillary tangles are homogeneously stained with fibrillar tau structures, which were most prominently stained with pT175/181, 12E8 (pS262/pS356), pS422, pS46, pS214 antibodies. Extracellular NFTs, which contain substantial filamentous tau, are most prominently stained with AT8 (pS199/pS202/pT205), AT100 (pT212/pS214), and PHF-1 (pS396/pS404) antibodies, which also stain intracellular NFT. The sequence of early tau phosphorylation suggests that there are events prior to filament formation that are specific to particular phosphorylated tau epitopes, leading to conformational changes and cytopathological alterations.

Keywords Epitope · Intraneuronal · Extraneuronal · Pretangle · Neurofibrillary tangle

Abbreviations AD Alzheimer's disease · *cdk5* cyclin dependent kinase 5 · *eNFT* extra-neuronal neurofibrillary tangle · *GSK-3 β* glycogen synthase kinase 3 β · *iNFT* intra-neuronal neurofibrillary tangle · *MAPK* mitogen-activated protein kinase · *MARK* microtubule affinity regulating kinase · *pre-NFT* pre-neurofibrillary tangle · *PHF* paired helical filament · *PKA* phosphorylation kinase A · *S* serine · *T* threonine

Introduction

Microtubule associated protein tau is a phosphoprotein that functions to stabilize microtubules and is expressed in both the fetal and adult human brain. Tau is highly phosphorylated in fetus, but unlike the fetal brain, tau is minimally phosphorylated in the normal adult brain [21, 25, 54]. However, tau is abnormally phosphorylated in Alzheimer's disease (AD) and is the main component in paired helical filaments (PHFs), and thus, neurofibrillary tangles (NFTs) [13, 14, 15, 19, 20, 24, 42, 44, 45]. Neurofibrillary tangles are one of the pathological signatures of AD and their presence correlates with severity of dementia [4, 11]. In AD, tau is phosphorylated at 19 specific amino acid sequences throughout its 441 amino acids.

The formation of a neurofibrillary tangle probably occurs in several steps. One approach to examining the issue of progression is to study morphological "stages" of NFTs: pre-NFT, intra-neuronal, and extra-neuronal NFT. Kimura et al. studied the development of phosphorylation of the tau molecule and showed that pre-NFTs were phosphorylated at serine (S) 199, S202, and S409, intra-neuronal NFTs were also phosphorylated at S396 and threonine (T) 231, and extra-neuronal NFTs are phosphorylated primarily at S396 [37]. In addition to morphological staging, it is also clear that NFTs occur in a stereotypical hierarchical distribution, with certain cytoarchitectural regions affected before others [3, 11]. For example, neurons

J.C. Augustinack · B.T. Hyman
Alzheimer's Unit, Department of Neurology,
Harvard Medical School, Massachusetts General Hospital,
Charlestown, MA 02129, USA

A. Schneider · E.-M. Mandelkow
Max-Planck-Unit for Structural Molecular Biology,
Notkestrasse 85, 22607 Hamburg, Germany

B.T. Hyman (✉)
114 16th St., Rm 2009, Alzheimer's Research Unit,
Harvard Medical School, Massachusetts General Hospital,
Charlestown, MA 02129, USA
e-mail: b_hyman@helix.mgh.harvard.edu,
Tel.: +1-617-7262299, Fax: +1-617-7241480

in layer II of the entorhinal cortex are among the first affected. In the current study, we used a panel of antibodies directed at a broad array of phospho-tau epitopes to examine AD cases with varying severity of neuropathological changes to establish a hierarchy of tau phosphorylation. We find a consistent pattern of tau phosphorylation in accord with a model of sequential phosphorylation.

Materials and methods

Patient selection

We studied 15 brains (eight female, seven male; ages 80.3 years \pm 15.0) received from the Alzheimer's Disease Research Center Brain Bank at Massachusetts General Hospital (Boston, Mass.) (Table 1). All cases were followed at the Neurology Clinic at Massachusetts General Hospital. Ten of the patients had a clinical diagnosis of Alzheimer's disease; one was multi-infarct dementia. All of the 11 pathological cases stained for phosphorylated tau and exhibited Alzheimer pathology, neurofibrillary tangles, and senile plaques. The mean brain weight for the Alzheimer's cases was 1089 g (\pm 186.13) (range 840–1175 g) and the mean duration of illness was 9.1 years (range 0–20 years). The mean post mortem interval in these cases averaged 12.7 h (\pm 6.5) with a range of 7–26 h. Further, four control brains, with no evidence of clinical dementia or other neurological disease, were examined and were negative for cerebral atrophy, neurofibrillary tangles, and senile plaques. The control group showed negative staining when stained with TG3, an antibody that recognizes the early stages of a neurofibrillary tangle. In the control group, the mean age was 62.7 (\pm 17.4) years old and mean brain weight was 1221.7 g (\pm 57.4).

Tissue processing

All cases were assessed by Khachaturian's criteria and CERAD guidelines [36, 47, 48] from paraffin sections using Bielschowski stain. All AD cases also met Reagan-NIA criteria. At autopsy, temporal lobe blocks were immersed in 4% peroxidate lysine paraformaldehyde and fixed for 48 h. After fixation, tissue was placed in 15% glycerol for cryoprotection. Temporal lobe blocks were sectioned coronally on a sliding microtome at 50 μ m, collected serially, and frozen at -20° C. All cases were stained with thionin, thioflavine S, PHF-1 [26], and anti-amyloid β (10D5) [31]. The control cases did not stain for thioflavine S or PHF-1 and did not meet the requirements outlined by the above criteria.

Tau antibodies

We studied the neurofibrillary tangles in Alzheimer's cases using 11 antibodies against phosphorylated tau. Each antibody recognizes a different epitope or a different conformational epitope (Fig. 1). The polyclonal antibodies raised against phosphorylated tau peptides and affinity purified are denoted by the residue number (e.g. pT153) and were produced in the Mandelkow laboratory [17, 32, 53]. Monoclonal antibodies against phospho-epitopes are denoted by their established names, e.g. AT8 [8, 23], AT100 [46], PHF-1 [27, 50], TG3 [34], and 12E8 [54]. AT8, AT100, PHF-1, TG3, and 12E8 are monoclonal antibodies used at dilutions 1:200, 1:100, 1:200, 1:25, and 1:500, respectively. pS46, pT153, pT175/181, pS214, pS262, pS422 are rabbit polyclonal antibodies that were used at dilutions 1:500, 1:80, 1:2000, 1:100, 1:20, and 1:200 respectively.

Immunocytochemistry

Human tissue was washed in 0.05 M tris buffered saline (TBS) to rid the tissue of glycerol solution. It was incubated with 0.5% Triton X-100 in 3% hydrogen peroxide to quench endogenous peroxide, then rinsed in TBS. The tissue was blocked using 5% instant non-fat dry milk in TBS for 2 h at room temperature and rinsed. All primary antibodies were incubated overnight at 4° C and diluted in 1.5% normal goat serum (NGS) (Jackson ImmunoResearch, West Grove, Pa.). The primary antibodies were removed and tissue was rinsed thoroughly in TBS. Secondary antibodies, goat anti-mouse and goat anti-rabbit, depending on the primary antibody, were diluted in 1.5% NGS at 1:200 and incubated for 1 h at room temperature (Jackson ImmunoResearch, West Grove, Pa.). Secondary antibodies were conjugated to horse radish peroxidase (HRP) or biotinylated goat anti-mouse or biotinylated goat anti-rabbit (Vector Laboratories, Burlingame, Calif.). Tissue was washed with TBS, and if biotinylated, incubated with ABC kit (Vector Labs, Burlingame, Calif.) for 1 h at room temperature. Finally, tissue was incubated with chromogen 3'-diaminobenzidine (DAB, Sigma, St. Louis, Mo.) in a solution of 0.003% DAB and 0.3% hydrogen peroxide for approximately 10 min. Tissue was rinsed thoroughly with TBS to clear the excess DAB. Sections were mounted, dried overnight, dehydrated in a series of ethanol solutions with increasing concentration, cleared in xylene and placed on coverslips with Permount (Fisher, Fair Lawn, N.J.). Negative control sections were processed with the same methods except that the primary antibody was either omitted or pre-absorbed. Occasional phospho-tau staining was observed in controls; however, it was minimal and restricted to layer II in entorhinal and perirhinal cortices. Positive controls, tissue that had previously been shown to express phosphorylated tau in neurofibrillary tangles in AD, were also included in all experiments.

Table 1 Results for 15 brains (AD Alzheimer's disease, MID multi-infarct dementia, YD years of dementia, BB stage Braak and Braak stage [11], BW brain weight (grams), C control, n/a not available)

Case	Age	Sex	Dx	BW	YD	BB stage	PMI	Death
1	79	F	AD	1175	6	VI	8	Dehydration
2	87	F	AD	1080	10	V	14	Coronary thrombosis
3	97	M	AD	1316	0	II	7	Stroke
4	104	F	AD	840	0	IV	7	Unknown
5	79	M	AD	1080	12	V	24	Unknown
6	83	M	AD	1015	10	V	12	Unknown
7	81	F	AD	1010	20	V	26	Unknown
8	84	F	AD	865	14	VI	10	Acute MI
9	86	M	AD	1440	n/a	III	9	Unknown
10	88	F	AD	937	15	V	12	Bronchopneumonia
11	86	M	MID	1220	4	III	10	Unknown
12	53	F	C	1190	–	–	18	Acute MI
13	88	F	C	1160	–	–	15	Respiratory failure
14	60	M	C	1287	–	–	39	Sepsis
15	50	M	C	1250	–	–	15	Bowel infarction

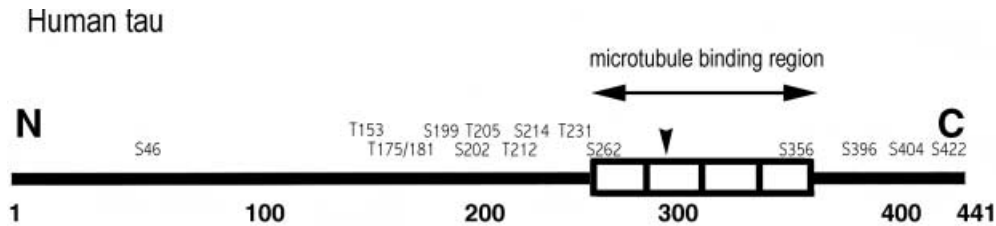


Fig. 1 The longest form of human tau is 441 amino acids. It contains four homologous repeats in the C-terminal half where microtubules bind tau. The second microtubule binding repeat contains the alternatively spliced exon 10 in human tau (*arrowhead*). This repeat, as well as two inserts near the N-terminus coded by exons 2 and 3 are absent from fetal tau. The phosphorylation sites or epitopes are labeled in the upper half of the figure (*S* serine, *T* threonine, *white rectangle* homologous repeat, *N* N terminal, *C* C terminal)

Anatomical areas

Since mesocortices and the hippocampal formation are the most vulnerable brain areas to neurofibrillary tangles, they were the focus of this study. Mesocortices include entorhinal cortex (area 28), perirhinal cortex (area 35) while the hippocampal formation contains parasubiculum, presubiculum, subiculum, CA1, CA2, CA3, CA4, and dentate gyrus. Additionally, temporal neocortices, Brodmann's area 36, 20, 21, and 22 were examined. The same groups of neurons were compared with regard to morphological and cytopathological observations of NFTs for the different tau antibodies. For example, entorhinal layer II was compared in each case with all the tau antibodies. Second, NFTs were compared across areas within each case. Different degrees of neuropathological changes among cases afforded the opportunity to compare morphological subtypes of NFTs in the context of the overall stage of neuropathological change.

Results

Morphological staging of NFT

Three types of neurofibrillary tangle-related neuropathological changes were examined: (1) pre-tangle phospho-tau aggregates, (2) iNFTs, and (3) eNFTs. We define a pre-NFT as a cell containing diffuse phospho-tau positive staining within the cytoplasm, sometimes including small punctate regions (Fig. 2A and B); the nucleus was detectable and the general cell morphology appeared normal. No condensed inclusions were noted. The cell soma has stainable cytoplasm and well preserved dendrites. INFTs contained aggregated filamentous structures within the cytoplasm that were positive for phospho-tau (Fig. 2C). The nucleus was present, but frequently displaced by the inclusion. Phospho-tau staining was often found in the proximal dendrites and axon hillock. Typically, the dendrites of an iNFT appeared deteriorated and were not as polarized to the apical and basal locations, but retained their positions (Fig. 2C). In an extra-neuronal NFT, a densely immunoreactive set of extracellular phospho-tau fibrils in the shape of a neuronal cell body was observed. The dendrites were collapsed, misaligned or absent. The cell soma revealed no stainable cytoplasm and appeared hollow because the darkly stained cytoskeleton and asso-

ciated proteins outlined the shape of the perimeter of the neuron (Fig. 2D). No nucleus was detected. Dense neuropil threads were often near eNFTs, representing the breakdown of dendritic and axonal structures.

Correlation of phospho-tau epitopes with morphological staging

We examined the different types of NFTs stained by each of 11 phospho-tau antibodies. Table 2 summarizes the hierarchical pattern of tau antibodies, their epitopes, putative kinases, and the cellular pathology that dominates for

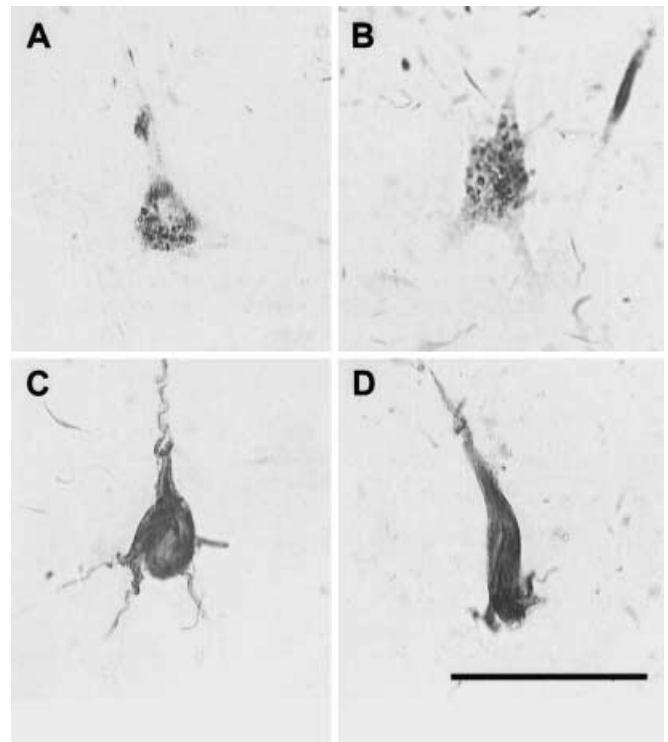


Fig. 2A–D Four examples of NFTs stained with TG3. In **A**, the neuron displays a unique phenomenon, the cell soma appears speckled with punctate regions of diffuse staining. Panels **A** and **B** represent pre-NFTs and both show punctate regions; the neurons shown here were observed in the entorhinal cortex. Note in **B** that the neuronal dendrites are numerous and viable. In addition, neurons typically contain a definable nucleus and even a nucleolus (**A** and **B**). An iNFT has a homogeneously stained cell soma and its basal dendrites are damaged slightly (**C**). An eNFT displays an atrophic neuron with no basal dendrites. The filamentous aggregations that have replaced the neuronal dendrites in an eNFT appear thicker because of the presence of PHF and no nucleus can be discerned either in **C** or **D**. Magnification bar=50 μ m

Table 2 The hierarchical pattern of tau antibodies, their epitopes, putative kinases, and the cellular pathology that dominates for a particular antibody

Antibody	Epitope ^[Ref]	Putative Kinases	pNFT	iNFT	eNFT
pT153	thr153 ^[34]	MAPK			
pS262	ser262 ^[23,24]	MARK			
TG3	thr231 ^[30]	CDC2, CDK5, GSK3b			
pT175/T181	thr175/181 ^[22]	MAPK			
12E8	ser262, ser 356 ^[1]	MARK, GSK3b			
pS422	ser422 ^[35]	MAPK			
pS46	ser46 ^[35]	GSK3b, MAPK			
pS214	ser214 ^[23]	PKA			
AT100	thr212, ser214 ^[36,37]	CDK5, GSK3b, MAPK, PKA			
AT8	ser199, ser202, thr205 ^[25,26]	CDK5, GSK3b, MAPK, PKA, PKC			
PHF-1	ser396, ser404 ^[28,29]	CDC2, CDK5, GSK3b, MAPK			

a particular antibody. Most of the sites covered in this study are serines or threonines, followed by a proline. This type of phosphorylation is characteristically elevated in Alzheimer tau [49], indicating that proline-directed serine/threonine kinases are overactive [e.g. mitogen-activated protein kinase (MAPK), glycogen synthase kinase 3 β (GSK-3 β), cyclin dependent kinase 5 (cdk5), and others], or that their corresponding phosphatases are inhibited. As a result, antibodies raised against Alzheimer tau are often directed against phospho-serine-proline or phospho-threonine-proline motifs. Such antibodies can therefore be used as diagnostic markers. Two other epitopes included in our studies were of a different nature but also elevated in AD: S214 can be phosphorylated by protein kinase A (PKA), and S262 by microtubule affinity regulating kinase (MARK) (or less efficiently by PKA); in both cases this phosphorylation is particularly effective in detaching tau from microtubules [45].

Unique pre-neurofibrillary tangles cytopathological alterations observed with pT153, pS262, and TG3 antibodies

pT153. pT153 antibody labeled neurons that contained pre-NFTs, intra-neuronal, and extra-neuronal NFTs (Fig. 3A); however the staining was dominated by the pretangle type. Dystrophic neurites or neuropil threads were observed in all cases, yet pT153-positive pre-NFT neurons are morphologically intact with a normal cellular integrity

and well preserved dendrites. We typically observed 10–15 punctate regions per neuron; each being roughly 2 μ m in diameter. Among the antibodies studied, neurons displayed this punctate staining pattern primarily using antibodies, pT153, pS262, and TG3.

pS262. Cases that were pS262-positive contained primarily pre-tangle NFT neurons (Fig. 3B), although iNFTs were also observed. We observed, as with pT153, that the neuronal integrity was healthy and that a nucleus was present. The basal and apical dendrites appeared intact, and for the most part, we did not observe folding or bending of dendrites. This antibody revealed punctate tau positive spherical inclusions in the pre-NFT neurons. The presence of these non-fibrillar punctate regions of tau, observed only in neurons with well-preserved neuronal somas, suggests that this is an early phenomenon.

TG3. This antibody against phosphorylated threonine 231 is a conformational epitope that labels all types of neurofibrillary tangles [34]. Pre-NFTs, iNFTs, and eNFTs were detected as well as neuropil threads. In pre-NFTs, the neuronal cytoplasm stained homogeneously, the cell soma had a healthy shape and displayed multiple outstretched dendrites. A select group of vulnerable neurons that reacted with TG3 displayed a punctate pattern that may represent endosomal and lysosomal staining. An example of a pre-NFT with the tau inclusions is illustrated in Fig. 2A and B where the nucleus and nucleolus can be discerned. TG3 also stained iNFTs and eNFTs in a pat-

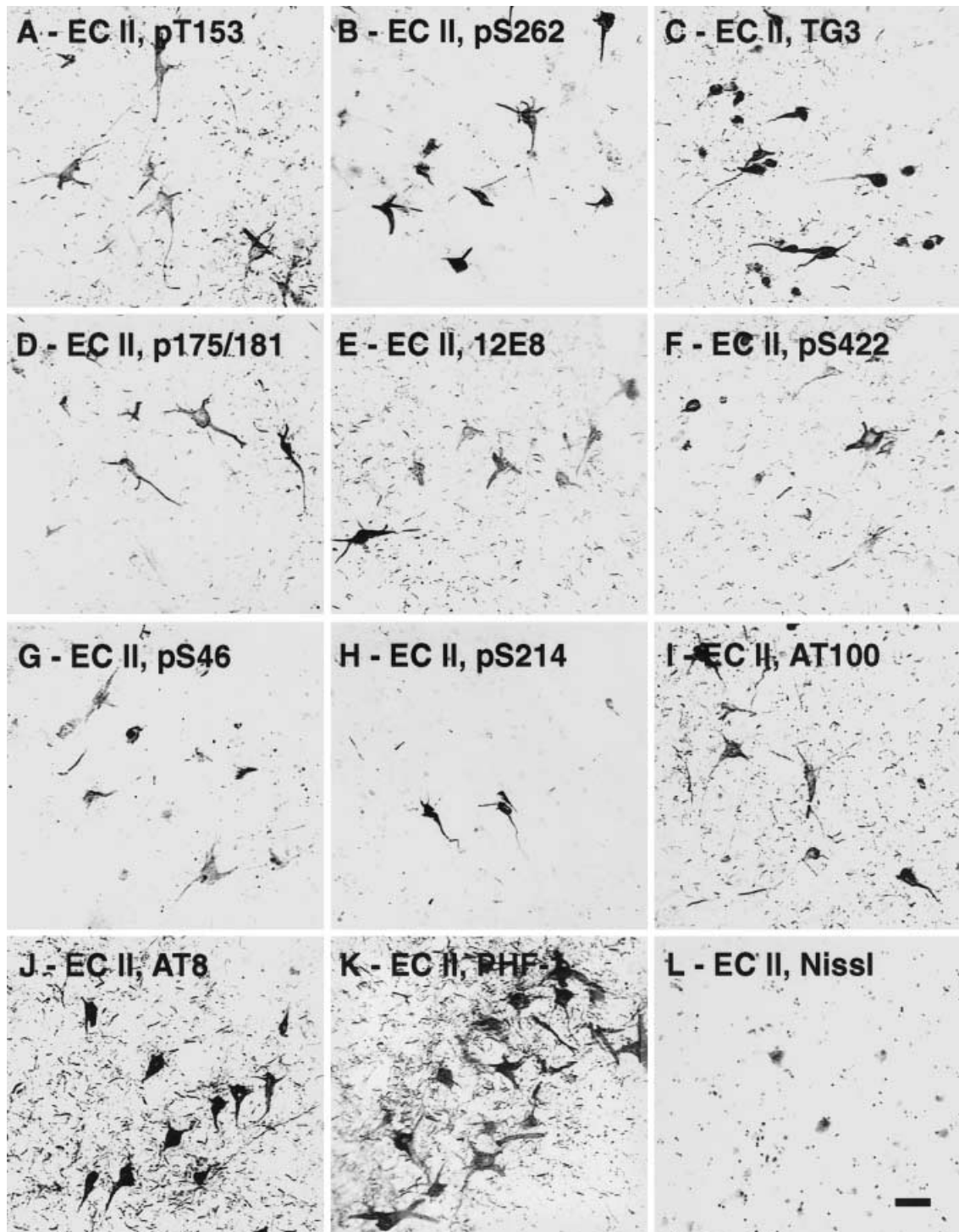


Fig.3 A-L An entorhinal layer II island from an 86-year-old patient with AD. Immunostaining with tau antibodies pT153 (A), pS262 (B), TG3 (C), pT175/pT181 (D), 12E8 (E), pS422 (F), pS46 (G), pS214 (H), AT100 (I), AT8 (J), PHF-1 (K), Nissl (L). Note the density of eNFTs in K and lack of neurons in the Nissl stain (L). Magnification bar=25 μ m

morphology and position. A moderate number of dystrophic neurites or neuropil threads were observed in all cases.

Antibodies T175/181, 12E8, pS422, pS46, and pS214 predominantly label intraneuronal NFTs

tern typical of other phospho-tau antibodies. As shown in Fig. 3C, basal dendrites exhibited a collapsed structure, although in this instance the apical dendrite maintained its

pT175/pT181. Neurons positive with antibody pT175/pT181 exhibited pre-tangle, intra-neuronal, and occasional

extra-neuronal NFTs; the pre-NFT morphologies were most prominent (Fig. 3D). The dendrites and their appropriate cellular locations were preserved in cells reacting with this antibody. Neuropil threads were observed consistently in all cases but the tissue was not densely stained for them.

12E8. This monoclonal antibody was raised against phosphorylated S262. This site is located in the KXGS motif of the first repeat whose phosphorylation effectively detaches tau from microtubules [6]. 12E8 recognizes this epitope, but also crossreacts with phosphorylated S356 (in the KXGS motif of the fourth repeat), and reacts weakly also with these epitopes in the unphosphorylated state [54]. The antibody stained pre-tangles, intra-neuronal, and extra-neuronal tangles (Fig. 3E), but without preference for a particular tangle type. The pre-tangle staining did not detect the punctate inclusions noted with pS262, pT153, and TG3, which was somewhat surprising considering that the major epitope for 12E8 is phosphorylated S262, but we note that 12E8 also recognizes phosphorylated S356 and unphosphorylated S262, which might explain the discrepancy. Moreover, 12E8 recognized far more iNFTs and eNFTs than the pS262 antibody, suggesting that subtle differences in epitope may greatly impact the amount of staining observed.

pS422. This antibody recognized predominantly cells that had lost their integrity. Primarily intra-neuronal and extra-neuronal NFTs (Fig. 3F) were observed with pS422, but staining of pre-tangles was rare. Neurons positive for pS422 usually did not display healthy dendrites or a normal dendritic position. Neuropil threads were moderately stained with pS422. Another antibody to this tau epitope, S422, has been produced by Goedert and colleagues and it is known to label less phospho-tau in the normal human brain than other phospho-tau antibodies [28].

pS46. Pre-tangle, intra-neuronal, and extra-neuronal tangles were observed with this antibody, but staining was dominated by iNFTs and eNFTs (Fig. 3G). The pre-tangle cells showed morphologically a more “advanced” stage, i.e. greater dendritic deterioration and a nucleus that was not as clear as observed, as with other phospho-tau antibodies, for example, TG3. We observed cell somas that were homogeneous, but lacked healthy dendrite morphology. Although most pS46-positive neurons displayed dystrophic dendrites, only few NTs were observed.

pS214. The antibody against phosphorylated S214 was generated because this site is phosphorylated by PKA (e.g. during mitosis) and strongly decreases the tau-microtubule interaction [12, 33]. The antibody immunostains occasional intra-neuronal and extra-neuronal NFTs but only rarely pre-tangles (Fig. 3H). The neuronal morphology was deteriorated, and the cell soma and dendrites were atrophied in most neurons. NTs were not densely stained with pS214, and overall the density of neurons that stain for pS214 was the lowest of all antibodies

tested. It has been shown in vitro that phosphorylation of S214 inhibits PHF formation [53], perhaps correlating with the observation that S214 immunostaining was not robust compared with other antibodies described here.

Antibodies AT100, AT8, and PHF-1 display prominent extraneuronal NFT staining

AT100. AT100 is directed against the doubly phosphorylated epitope T212 and S214 which can be created by sequential phosphorylation with GSK-3 β and PKA; it is one of the most specific antibodies against Alzheimer tau [29, 57]. The antibody stained both iNFT and eNFTs. In iNFTs, AT100-positive neurons revealed dendritic arbors, while in the case of eNFTs, AT100-positive neurons displayed collapsed basal dendrites and often had many surrounding neuropil threads (Fig. 3I). As observed with other antibodies, eNFTs created the appearance of hollow cell somas.

AT8. AT8, the most prominent of the AT-series of monoclonal antibodies [46], recognizes a doubly phosphorylated epitope including S199, S202, and T205 [8, 23]. It stained iNFTs and eNFTs. Intense staining of extraneuronal tangles was dominant in advanced cases, whereas pre-NFTs were rarely observed. With this antibody, iNFTs typically presented collapsed dendrites and revealed dense neuropil thread staining (Fig. 3J). Remarkably, select neurons still contained stainable cytoplasm, but these were rarely observed. The eNFTs had an empty interior and contained no stainable cytoplasm (Fig. 3J).

PHF-1. PHF-1 is also directed against a doubly phosphorylated epitope, S396 and S404 [27, 39]. Its staining pattern showed intense NTs and predominance of eNFTs in advanced cases (Fig. 3K). Numerous intra-neuronal tangles were observed, but these were less robustly stained than the eNFT. PHF-1 labeled many NFTs and NTs across many areas, and is the densest of all antibodies tested, especially in severe AD cases. An adjacent section stained for Nissl substance showed few viable neurons in this AD case (Fig. 3L).

Morphological and biochemical phenotypes correlate with regional patterns of vulnerability for NFTs

Pre-NFT tau antibodies (pT153, pS262, TG3). These antibodies predominantly stained pre-NFTs and to a lesser degree iNFTs. Layer II entorhinal islands and layer IV were densely stained in moderate cases (Braak stage III–IV), but much less in severe AD cases. The neighboring mesocortical perirhinal cortex contained NFTs in layers II and III organized in columns. In the hippocampal formation, CA1 and subicular neurons were immunoreactive, but other areas such as CA2 and CA3 were less densely stained. CA4 and granules cells of the dentate gyrus were also not densely stained, but if aggregation was observed,

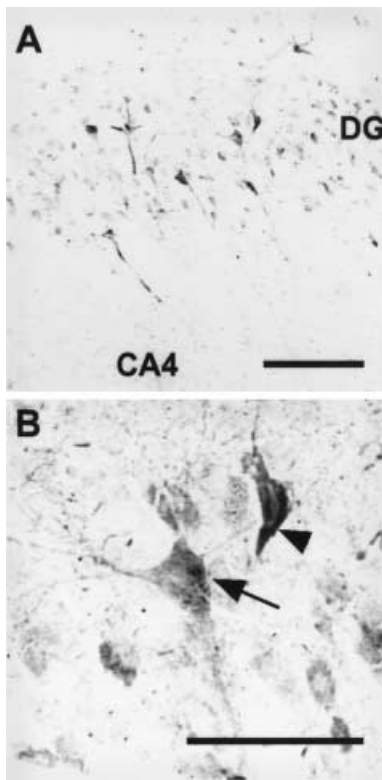


Fig. 4A,B AT100 staining in dentate gyrus contains moderate NFTs and hippocampal field CA4 contains sparse NFTs in this 83-year-old patient with 10 years of dementia (A). Neurofibrillary tangles are depicted with filamentous tau (*arrowhead*) and punctate tau (*arrow*) in B. Magnification bar=100 μ m

it was either pre-NFT or intra-neuronal. Intra-neuronal NFTs were sparsely present in layers III and V of temporal neocortical areas 36, 20, 21, and 22.

Intra-neuronal NFT tau antibodies (pT175/181, 12E8, pS422, pS214, and pS46). Entorhinal layer II islands were immunostained with all of the above-mentioned antibodies; however, the immunoreactivity was not as robust as the antibodies that stain primarily pre-NFTs (pT153, pS262, and TG3) nor the antibodies that stain primarily eNFTs (AT100, AT8, and PHF-1). The supragranular layers of the perirhinal cortex revealed similar staining as the entorhinal islands. Moderate cases, nonetheless, revealed substantial immunostaining compared with the severe cases. Immunostaining in the temporal neocortical areas yielded easily detectable reactivity in moderate cases, but more reactivity in the severe cases. Likewise, the hippocampal areas subiculum and CA1 contained NFTs in moderate and severe cases whereas little staining was observed in CA2–CA4 and dentate gyrus.

Intra- and extra-neuronal NFT tau antibodies (AT100, AT8, and PHF-1). Entorhinal layer II was densely immunostained with AT100, AT8, and PHF-1 in Braak stages IV, V, and VI. The moderate, and especially the severe, cases revealed strong staining in layer II, but in mild

cases the immunoreactivity did not show the dense eNFTs using these antibodies (Fig. 3K). Similarly, in adjacent perirhinal cortex, the presence of NFTs in columns varied and depended on the severity of the cases. The hippocampal fields CA1 and subiculum contained heavy eNFT staining, and there was even immunostaining in CA2–CA4 and dentate gyrus (Fig. 4A and B), containing intra-neuronal neurofibrillary tangles. The severe cases exhibited dense staining of all neurofibrillary tangle types in layers III and V of the temporal neocortices. In general, in severe AD cases (i.e. stage V or VI) [11], these tau antibodies labeled dense eNFTs to the greatest extent.

Discussion

There is a hierarchy of NFTs in various brain areas, with some areas affected prior to others [3, 11]. In the current study, we suggest that there is also a consistent pattern of tau phosphorylation that corresponds to the degree of neuronal cytopathology. We examined three morphological types of NFTs, pre-NFTs, iNFTs, and eNFTs according to the phosphorylation sites of tau as seen by specific monoclonal or peptide antibodies, and compared them with the severity of neuropathological changes. First, these data suggest that tau antibodies pT153, pS262, TG3, and pT175/pT181 are immunoreactive at an early step in the development of an NFT, and may begin with unique punctate inclusions that appear to precede fibrillar NFTs. Second, tau antibodies 12E8, pS422, pS46, and pS214 are immunoreactive in the next step of NFT formation (i.e. iNFT). Third, tau antibodies AT100, AT8, and PHF-1 are present in iNFT and remain present in the last step in the progression in an eNFT. Particular epitopes may be lost or covered during evolution of the lesion, especially as eNFTs form. Finally, these data suggest that the development of an NFT occurs in a stepwise fashion with pre-NFT, iNFT, and eNFT types as cellular stages throughout the evolution of an NFT. Kimura et al. [37] examined fewer phosphorylation sites, S199, 202, 409, 422, 396, and T231 and used different antibodies to these epitopes. Their results are similar in that S396 phosphorylation is present on eNFTs or ghost tangles in both studies. However, Kimura et al. observed that T231 immunoreactive is exclusively on eNFTs, whereas we and others [34] observed a range of NFT types with this antibody TG3. Furthermore, Kimura et al. reported that pre-NFT contain S199 and 202, whereas in our data these epitopes were more prominent on iNFT and even eNFT (e.g. AT8 immunostaining, which is widely used as a marker of NFT).

Of particular interest to us was the observations of small punctate inclusion in pre-tangles. These punctate regions were observed occasionally in PHF-1 and AT8 tau stains, but were most prominent in TG3, pT153, and pS262 antibody stains. Since the punctate, but not filamentous, inclusions were observed in neurons with a nucleus and a nucleolus present, it is likely an early event in NFT development. Further, these intraneuronal cytoplasmic

mic aggregations, possibly early endosomal or lysosomal compartments, may be a result of abnormally phosphorylated tau or another mechanism involving amyloid beta peptide. This type of inclusion was observed only in neuronal populations already known to be vulnerable for NFT formation, such as entorhinal layers II, III, IV, perirhinal layers II, III, V, hippocampal CA1, and temporal neocortical layers III and V. Neurons carrying pre-NFTs were most prominent in mild cases (Braak and Braak stage <IV) and were the only type of cells to contain the tau-positive punctate regions. The punctate inclusions described in this report are different from the argyrophilic grains previously described by Braak and Braak [9, 10], which are small spindled shaped grains that are extracellular. In addition, the tau inclusions are different from Hirano bodies that are eosinophilic, rod-like structures occasionally observed in AD [30]. Our tau-positive inclusions are also different from granulovacuolar degeneration in that there is no vacuole surrounding the inclusion and it is observed in mesocortices as well as the hippocampus, whereas granulovacuolar lesions are primarily found in the CA1 and subicular fields in the hippocampus. Nuclear staining was not observed; however, punctate regions were observed near and on top of the nucleus. In the case of Huntington's disease and other diseases caused by trinucleotide repeat expansions, the encoded proteins containing poly-Gln stretches have been found both in the cytosol and in the nucleus [2, 35, 40]. However, this is not the case with tau aggregates in AD.

Kinases that phosphorylate tau have become a major target in attempts to understand why tau becomes highly phosphorylated in AD. MAPK has been shown to phosphorylate several tau sites in vitro. Phosphopeptide mapping and sequencing shows that the most pronounced sites are T153 and S235; other sites with lower but roughly comparable weights include T175, T181, S422, S46, T50, T212, S199, S202, T205, S396, and S404 [33]. Cdk5 induces most prominent phosphorylation at S235, S202, S404, and with lower intensity at S199, T212, and T205 [5, 33]. GSK-3 β shows the highest phosphorylation at S404 and S396, followed by T50 and S46, and weakly at S199, S202, T205, and T212 [5, 18, 33, 43, 55, 57]. Given these data, MAPK would be expected to induce the most visible interaction with antibody pT153, AT-180, and with lesser weight AT-8 and PHF-1; cdk5 would generate the most pronounced reaction with AT-8, and GSK3 β would highlight the PHF-1 epitope. But we note that many of the pathological epitopes on tau are generated by sequential phosphorylation of a pair of phosphorylated residues by the same kinase or two different kinases (e.g. first S202, later T205 for AT-8; first S404, later S396 for PHF-1; first S235, later S231 for AT-180; first T212, later S214 for AT-100). A consequence is that the most pronounced phosphorylation site of a kinase does not necessarily correspond to the most visible antibody reaction. An example is S235, which is strongly phosphorylated by cdk5, but the AT-180 reaction is not induced because S231 shows low phosphorylation so that the most apparent antibody staining is that of AT-8.

Phosphorylation tends to weaken the tau-microtubule interaction. However, the effect is not very pronounced for SP or TP sites, the targets of proline-directed kinases MAPK, cdk5, and GSK-3 β . Conversely, MARK and PKA phosphorylate S262 in the repeat domain and S214 in the flanking domain before the repeats, and both phosphorylation sites strongly inhibit tau-microtubule interactions [8, 17, 22, 33, 41, 52]. From the type of kinase that phosphorylate these tau epitopes (Table 2) and the tau NFT hierarchy established in this report, it is plausible that the combination and number of kinases predicts and causes the type of neurofibrillary tangle. For example, these data are consistent with the idea that residues S262, T153, and T175/T181 are phosphorylated early in the pathological process, implicating MARK and MAPK, respectively. At a later stage, the reaction of antibodies AT-8, AT-100, and PHF-1 points to a pronounced activity of GSK-3 β and cdk5 because the epitopes are efficiently phosphorylated by this kinase in vitro.

One of the earliest phospho-tau related changes is phosphorylation of S262. As shown by Schneider et al. [53] the same sites that most strongly inhibit tau-microtubule interactions (S262 and S214) also inhibit PHF aggregation in vitro most effectively, whereas proline-directed sites have a smaller effect, but also inhibitory [6, 7, 16, 17, 33]. Indeed, our data suggest that pS262 tau may form non-fibrillar aggregates in pre-NFT. What then causes aggregation into a fibrillar form? One possibility is that additional phosphorylation events (e.g. pT175/181) may be necessary. Another possibility is that PHF aggregation may not depend on phosphorylation, per se, and instead be initiated directly on a molecular scaffold such as the microtubule surface overloaded with excess tau [1]. This might be accompanied by a change in tau's conformation which is detected by certain antibodies, such as TG3 [34] and Alz50 [56]. In either case, it seems possible that PHF-tau continues to be phosphorylated after aggregation as suggested by the change in phospho-epitopes observed in the current study and by the tight association of multiple kinases, including MAPK [33, 38], GSK3 β [18, 57], cdk5 [5, 51], MARK [16, 17], and PKA [57], with fibrillar iNFT. This would also agree with the finding that PHFs aggregated from recombinant tau in vitro can still be phosphorylated by proline-directed kinases at SP or TP motifs, as well as by MARK and PKA at S262 and S214 [53].

Sequential phosphorylation makes the issue of tau phosphorylation even more complex. It has been shown that sequential phosphorylation in vitro is required at T212 and S214 by GSK-3 β and PKA, respectively. It is only when a specific order of phosphorylation occurs (S199, 202, T231 \Rightarrow T212 \Rightarrow S214) that the AT100 epitope is formed [57]. It is highly likely that other such cascades exist for other tau epitopes, but have not been examined in as much detail as AT100. In this report, our observations indicate that pS214 recognizes an earlier stage of PHF aggregation than AT100. The discrepancy between the data of Zheng-Fischhofer et al. and the data in the present results could suggest that there are two distinct mecha-

nisms of phosphorylation. First, an early one in which only PKA phosphorylates S214 and this then prevents phosphorylation of T212 and the generation of the AT100 epitope. Second, a later phosphorylation mechanism where GSK-3 β phosphorylates T212, then PKA phosphorylates S214, and thus, this phosphorylation completes the AT100 epitope. The earlier phosphorylation of S214 is in agreement with the fact that this phosphorylation detaches tau from microtubules, and therefore, makes tau available for PHF formation. A similar issue is the relationship between antibodies 12E8 and pS262 that recognize the same epitope, pS262, and, yet, they occur in different stages. This is due, perhaps, to different affinities of antibodies. Another possibility is that there is crossreactivity of 12E8 with pS356 (in a closely similar KIGS motif) and to a lesser extent with unphosphorylated S262, which is not the case for the pS262 because it only recognizes this epitope. It is noteworthy that among the two sites pS214 and pS262 that are known to strongly decrease tau's affinity for microtubules, only pS262 appears to be high at early stages, consistent with the notion that detachment of tau comes before PHF aggregation occurs. However, this preference of an early stage is seen only with the antibody pS262 and not with 12E8, which illustrates that the epitopes and conformations of these antibodies must be different.

In summary, our results suggest that there is an evolution of tau phosphorylation in AD. A healthy neuron develops punctate phospho-tau inclusions, becomes a pre-NFT which gives rise to a filamentous intra-cellular inclusion. Eventually the neuron dies and an extra-neuronal NFT, or ghost tangle remains. During this progression additional phospho-epitopes appear. These may act as markers for the sequential activation of kinases as neuronal cytopathology proceeds.

Acknowledgement We thank Dr. Peter Davies for antibodies PHF-1 and TG3.

References

- Ackmann M, Wiech H, Mandelkow E (2000) Nonsaturable binding indicates clustering of tau on the microtubule surface in a paired helical filament-like conformation. *J Biol Chem* 275:30335–30343
- Andrew SE, Goldberg YP, Kremer B, Telenius H, Theilmann J, Adam S, Starr E, Squitieri F, Lin B, Kalchman MA et al. (1993) The relationship between trinucleotide (CAG) repeat length and clinical features of Huntington's disease. *Nat Genet* 4:398–403
- Arnold SE, Hyman BT, Flory J, Damasio AR, Van Hoesen GW (1991) The topographical and neuroanatomical distribution of neurofibrillary tangles and neuritic plaques in the cerebral cortex of patients with Alzheimer's disease. *Cereb Cortex* 1:103–116
- Arriagada PV, Growdon JH, Hedley-Whyte ET, Hyman BT (1992) Neurofibrillary tangles but not senile plaques parallel duration and severity of Alzheimer's disease. *Neurology* 42:631–639
- Baumann K, Mandelkow EM, Biernat J, Piwnica-Worms H, Mandelkow E (1993) Abnormal Alzheimer-like phosphorylation of tau-protein by cyclin-dependent kinases cdk2 and cdk5. *FEBS Lett* 336:417–424
- Biernat J, Gustke N, Drewes G, Mandelkow EM, Mandelkow E (1993) Phosphorylation of Ser262 strongly reduces binding of tau to microtubules: distinction between PHF-like immunoreactivity and microtubule binding. *Neuron* 11:153–163
- Biernat J, Mandelkow EM (1999) The development of cell processes induced by tau protein requires phosphorylation of serine 262 and 356 in the repeat domain and is inhibited by phosphorylation in the proline-rich domains. *Mol Biol Cell* 10:727–740
- Biernat J, Mandelkow EM, Schroter C, Lichtenberg-Kraag B, Steiner B, Berling B, Meyer H, Mercken M, Vandermeeren A, Goedert M, et al. (1992) The switch of tau protein to an Alzheimer-like state includes the phosphorylation of two serine-proline motifs upstream of the microtubule binding region. *Embo J* 11:1593–1597
- Braak H, Braak E (1987) Argyrophilic grains: characteristic pathology of cerebral cortex in cases of adult onset dementia without Alzheimer changes. *Neurosci Lett* 76:124–127
- Braak H, Braak E (1989) Cortical and subcortical argyrophilic grains characterize a disease associated with adult onset dementia. *Neuropathol Appl Neurobiol* 15:13–26
- Braak H, Braak E (1991) Neuropathological staging of Alzheimer-related changes. *Acta Neuropathol* 82:239–259
- Brandt R, Lee G, Teplow DB, Shalloway D, Abdel-Ghany M (1994) Differential effect of phosphorylation and substrate modulation on tau's ability to promote microtubule growth and nucleation. *J Biol Chem* 269:11776–11782
- Crowther T, Goedert M, Wischik CM (1989) The repeat region of microtubule-associated protein tau forms part of the core of the paired helical filament of Alzheimer's disease. *Ann Med* 21:127–132
- Crowther RA, Olesen OF, Jakes R, Goedert M (1992) The microtubule binding repeats of tau protein assemble into filaments like those found in Alzheimer's disease. *FEBS Lett* 309:199–202
- Crowther RA, Olesen OF, Smith MJ, Jakes R, Goedert M (1994) Assembly of Alzheimer-like filaments from full-length tau protein. *FEBS Lett* 337:135–138
- Drewes G, Ebnet A, Preuss U, Mandelkow EM, Mandelkow E (1997) MARK, a novel family of protein kinases that phosphorylate microtubule-associated proteins and trigger microtubule disruption. *Cell* 89:297–308
- Drewes G, Trinczek B, Illenberger S, Biernat J, Schmitt-Ulms G, Meyer HE, Mandelkow EM, Mandelkow E (1995) Microtubule-associated protein/microtubule affinity-regulating kinase (p110mark). A novel protein kinase that regulates tau-microtubule interactions and dynamic instability by phosphorylation at the Alzheimer-specific site serine 262. *J Biol Chem* 270:7679–7688
- Godemann R, Biernat J, Mandelkow E, Mandelkow EM (1999) Phosphorylation of tau protein by recombinant GSK-3 β : pronounced phosphorylation at select Ser/Thr-Pro motifs but no phosphorylation at Ser262 in the repeat domain. *FEBS Lett* 454:157–164
- Goedert M (1993) Tau protein and the neurofibrillary pathology of Alzheimer's disease. *Trends Neurosci* 16:460–465
- Goedert M, Crowther RA (1989) Amyloid plaques, neurofibrillary tangles and their relevance for the study of Alzheimer's disease. *Neurobiol Aging* 10:405–406; 412–414
- Goedert M, Jakes R, Crowther RA, Cohen P, Vanmechelen E, Vandermeeren M, Cras P (1994) Epitope mapping of monoclonal antibodies to the paired helical filaments of Alzheimer's disease: identification of phosphorylation sites in tau protein. *Biochem J* 301:871–877
- Goedert M, Jakes R, Qi Z, Wang JH, Cohen P (1995) Protein phosphatase 2 A is the major enzyme in brain that dephosphorylates tau protein phosphorylated by proline-directed protein kinases or cyclic AMP-dependent protein kinase. *J Neurochem* 65:2804–2807
- Goedert M, Jakes R, Vanmechelen E (1995) Monoclonal antibody AT8 recognises tau protein phosphorylated at both serine 202 and threonine 205. *Neurosci Lett* 189:167–169

24. Goedert M, Sisodia SS, Price DL (1991) Neurofibrillary tangles and beta-amyloid deposits in Alzheimer's disease. *Curr Opin Neurobiol* 1:441-447
25. Goedert M, Wischik CM, Crowther RA, Walker JE, Klug A (1988) Cloning and sequencing of the cDNA encoding a core protein of the paired helical filament of Alzheimer disease: identification as the microtubule-associated protein tau. *Proc Natl Acad Sci USA* 85:4051-4055
26. Greenberg SG, Davies P (1990) A preparation of Alzheimer paired helical filaments that displays distinct tau proteins by polyacrylamide gel electrophoresis. *Proc Natl Acad Sci USA* 87:5827-5831
27. Greenberg SG, Davies P, Schein JD, Binder LI (1992) Hydrofluoric acid-treated tau PHF proteins display the same biochemical properties as normal tau. *J Biol Chem* 267:564-569
28. Hasegawa M, Jakes R, Crowther RA, Lee VM, Ihara Y, Goedert M (1996) Characterization of mAb AP422, a novel phosphorylation-dependent monoclonal antibody against tau protein. *FEBS Lett* 384:25-30
29. Hoffmann R, Lee VMY, Leight S, Varga I, Otvos L Jr (1997) Unique Alzheimer's disease paired helical filament specific epitopes involve double phosphorylation at specific sites. *Biochemistry* 36:8114-8124
30. Hirano A, Dembitzer HM, Kurland LT, Zimmerman HM (1968) The fine structure of some intraganglionic alterations. Neurofibrillary tangles, granulovacuolar bodies and "rod-like" structures as seen in Guam amyotrophic lateral sclerosis and parkinsonism-dementia complex. *J Neuropathol Exp Neurol* 27:167-182
31. Hyman BT, Tanzi RE (1992) Amyloid, dementia and Alzheimer's disease. *Curr Opin Neurol Neurosurg* 5:88-93
32. Illenberger S, Drewes G, Trinczek B, Biernat J, Meyer HE, Olmsted JB, Mandelkow EM, Mandelkow E (1996) Phosphorylation of microtubule-associated proteins MAP2 and MAP4 by the protein kinase p110mark. Phosphorylation sites and regulation of microtubule dynamics. *J Biol Chem* 271:10834-10843
33. Illenberger S, Zheng-Fischhofer Q, Preuss U, Stamer K, Baumann K, Trinczek B, Biernat J, Godemann R, Mandelkow EM, Mandelkow E (1998) The endogenous and cell cycle-dependent phosphorylation of tau protein in living cells: implications for Alzheimer's disease. *Mol Biol Cell* 9:1495-1512
34. Jicha GA, Lane E, Vincent I, Otvos L, Jr., Hoffmann R, Davies P (1997) A conformation- and phosphorylation-dependent antibody recognizing the paired helical filaments of Alzheimer's disease. *J Neurochem* 69:2087-2095
35. Jou YS, Myers RM (1995) Evidence from antibody studies that the CAG repeat in the Huntington disease gene is expressed in the protein. *Hum Mol Genet* 4:465-469
36. Khachaturian ZS (1985) Diagnosis of Alzheimer's disease. *Arch Neurol* 42:1097-1105
37. Kimura T, Ono T, Takamatsu J, Yamamoto H, Ikegami K, Kondo A, Hasegawa M, Ihara Y, Miyamoto E, Miyakawa T (1996) Sequential changes of tau-site-specific phosphorylation during development of paired helical filaments. *Dementia* 7:177-181
38. Knowles RB, Chin J, Ruff CT, Hyman BT (1999) Demonstration by fluorescence resonance energy transfer of a close association between activated MAP kinase and neurofibrillary tangles: implications for MAP kinase activation in Alzheimer disease. *J Neuropathol Exp Neurol* 58:1090-1098
39. Lang E, Szendrei GI, Lee VM, Otvos L Jr (1992) Immunological and conformation characterization of a phosphorylated immunodominant epitope on the paired helical filaments found in Alzheimer's disease. *Biochem Biophys Res Commun* 187:783-790
40. Li XJ, Li SH, Sharp AH, Nucifora FC, Jr., Schilling G, Lanhana A, Worley P, Snyder SH, Ross CA (1995) A huntingtin-associated protein enriched in brain with implications for pathology. *Nature* 378:398-402
41. Litersky JM, Johnson GV, Jakes R, Goedert M, Lee M, Seubert P (1996) Tau protein is phosphorylated by cyclic AMP-dependent protein kinase and calcium/calmodulin-dependent protein kinase II within its microtubule-binding domains at Ser-262 and Ser-356. *Biochem J* 316:655-660
42. Mandelkow EM, Biernat J, Drewes G, Steiner B, Lichtenberg-Kraag B, Wille H, Gustke N, Mandelkow E (1993) Microtubule-associated protein tau, paired helical filaments, and phosphorylation. *Ann NY Acad Sci* 695:209-216
43. Mandelkow EM, Drewes G, Biernat J, Gustke N, Van Lint J, Vandenhede JR, Mandelkow E (1992) Glycogen synthase kinase-3 and the Alzheimer-like state of microtubule-associated protein tau. *FEBS Lett* 314:315-321
44. Mandelkow EM, Mandelkow E (1994) Tau protein and Alzheimer's disease. *Neurobiol Aging* 15:S85-86
45. Mandelkow EM, Mandelkow E (1998) Tau in Alzheimer's disease. *Trends Cell Biol* 8:425-427
46. Mercken M, Vandermeeren M, Lubke U, Six J, Boons J, Van de Voorde A, Martin JJ, Gheuens J (1992) Monoclonal antibodies with selective specificity for Alzheimer Tau are directed against phosphatase-sensitive epitopes. *Acta Neuropathol* 84:265-272
47. Mirra SS (1997) Neuropathological assessment of Alzheimer's disease: the experience of the Consortium to Establish a Registry for Alzheimer's Disease. *Int Psychogeriatr* 9:263-268; 269-272
48. Mirra SS, Heyman A, McKeel D, Sumi SM, Crain BJ, Brownlee LM, Vogel FS, Hughes JP, van Belle G, Berg L (1991) The Consortium to Establish a Registry for Alzheimer's Disease (CERAD). II. Standardization of the neuropathologic assessment of Alzheimer's disease. *Neurology* 41:479-486
49. Morishima-Kawashima M, Hasegawa M, Takio K, Suzuki M, Yoshida H, Watanabe A, Titani K, Ihara Y (1995) Hyperphosphorylation of tau in PHF. *Neurobiol Aging* 16:365-380
50. Otvos L Jr, Feiner L, Lang E, Szendrei GI, Goedert M, Lee VM (1994) Monoclonal antibody PHF-1 recognizes tau protein phosphorylated at serine residues 396 and 404. *J Neurosci Res* 39:669-673
51. Patrick GN, Zukerberg L, Nikolic M, de la Monte S, Dikkes P, Tsai LH (1999) Conversion of p35 to p25 deregulates Cdk5 activity and promotes neurodegeneration. *Nature* 402:615-622
52. Robertson J, Loviny TL, Goedert M, Jakes R, Murray KJ, Anderton BH, Hanger DP (1993) Phosphorylation of tau by cyclic-AMP-dependent protein kinase. *Dementia* 4:256-263
53. Schneider A, Biernat J, von Bergen M, Mandelkow E, Mandelkow EM (1999) Phosphorylation that detaches tau protein from microtubules (Ser262, Ser214) also protects it against aggregation into Alzheimer paired helical filaments. *Biochemistry* 38:3549-3558
54. Seubert P, Mawal-Dewan M, Barbour R, Jakes R, Goedert M, Johnson GV, Litersky JM, Schenk D, Lieberburg I, Trojanowski JQ et al. (1995) Detection of phosphorylated Ser262 in fetal tau, adult tau, and paired helical filament tau. *J Biol Chem* 270:18917-18922
55. Sperber BR, Leight S, Goedert M, Lee VM (1995) Glycogen synthase kinase-3 beta phosphorylates tau protein at multiple sites in intact cells. *Neurosci Lett* 197:149-153
56. Vincent IJ, Davies P (1990) Phosphorylation characteristics of the A68 protein in Alzheimer's disease. *Brain Res* 531:127-135
57. Zheng-Fischhofer Q, Biernat J, Mandelkow EM, Illenberger S, Godemann R, Mandelkow E (1998) Sequential phosphorylation of Tau by glycogen synthase kinase-3beta and protein kinase A at Thr212 and Ser214 generates the Alzheimer-specific epitope of antibody AT100 and requires a paired-helical-filament-like conformation. *Eur J Biochem* 252:542-552